Widespread shortening of 3' untranslated regions and increased exon inclusion are evolutionarily conserved features of innate immune responses to infection

Athma A. Pai[a,1,2], Golshid Baharian[b,c,1], Ariane Pagé Sabourin[c], Jessica F. Brinkworth[b,c,d], Yohann Nédélec[b,c], Joseph W. Foley[e], Jean-Christophe Grenier[c], Katherine J. Siddle[f], Anne Dumaine[c], Vania Yotova[c], Zachary P. Johnson[g,h], Robert E. Lanford [i], Christopher B. Burge[a,j], Luis B. Barreiro[c,k,2]

[a]Department of Biology, Massachusetts Institute of Technology, Cambridge, MA, USA

[b]Department of Biochemistry, Faculty of Medicine, University of Montreal, Montreal, QC, Canada

[c]Sainte-Justine Hospital Research Centre, Montreal, QC, Canada

[d]Department of Anthropology, University of Illinois, Urbana-Champaign, IL, USA

[e]Department of Pathology, Stanford University School of Medicine, Stanford, CA, USA

[f]Department of Organismic and Evolutionary Biology, FAS Center for Systems Biology, Harvard University, Cambridge, MA, USA

[g]Yerkes National Primate Research Center, Emory University, Atlanta, GA 30322, USA

[h]Department of Human Genetics, Emory University School of Medicine, Atlanta, GA 30322, USA

[i]Texas Biomedical Research Institute, Department of Virology and Immunology, San Antonio, TX, USA.

[j]Department of Biological Engineering, Massachusetts Institute of Technology, Cambridge, MA, USA

[k]Department of Pediatrics, Faculty of Medicine, University of Montreal, Montreal, QC, Canada

[1]These authors contributed equally to this work.

[2]To whom correspondence should be addressed. E-mail: athma@mit.edu and luis.barreiro@umontreal.ca

ABSTRACT

The contribution of pre-mRNA processing mechanisms to the regulation of immune responses remains poorly studied despite emerging examples of their role as regulators of immune defenses. Here, we used mRNA sequencing to quantify gene expression and isoform abundances in primary macrophages from 60 individuals, before and after infection with two live bacteria. In response to both bacteria we identified thousands of genes that significantly change isoform usage in response to infection, and found global shifts towards (*i*) the inclusion of cassette exons and (*ii*) shorter 3' UTRs. Using complementary data collected in non-human primates, we show that these features are evolutionarily conserved among primates. Finally, our results suggest that the pervasive usage of shorter 3' UTRs is a mechanism for particular genes to evade repression by immune-activated miRNAs. Collectively, our results show that dynamic changes in RNA processing play a key role in the regulation of innate immune responses.

INTRODUCTION

Innate immune responses depend on robust and coordinated gene expression programs involving the transcriptional regulation of thousands of genes (Huang et al. 2001; Smale 2010; Medzhitov and Horng 2009). These regulatory cascades start with the detection of microbial-associated products by pattern recognition receptors, which include Toll Like Receptors (TLRs), NOD-like receptors and specific C-type lectins (Medzhitov and Janeway 1998; Kawai and Akira 2010). These initial steps are followed by the activation of key transcription factors (e.g., NF-κB and interferon regulatory factors) that orchestrate the inflammatory and/or antiviral response signals involved in pathogen clearance and the subsequent development of appropriate adaptive immune responses (Medzhitov and Janeway 1998).

Although much attention has been devoted to characterizing transcriptional changes in response to infectious agents or other immune stimuli, we still know remarkably little about the contribution of post-transcriptional changes – specifically, changes in alternative pre-mRNA processing – to the regulation of the immune system (Lynch 2004; Martinez and Lynch 2013; Alasoo et al. 2015). Alternative splicing can impact cellular function by creating distinct mRNA transcripts from the same gene, which may encode unique proteins that have distinct or opposing functions. For instance, in human and mouse cells, several alternatively spliced forms of genes involved in the TLR pathway have been shown to function as negative regulators of TLR signaling in order to prevent uncontrolled inflammation (Rao et al. 2005; Wells et al. 2006; O'Connor et al. 2015). Additionally, several in-depth studies of individual genes suggest that alternative splicing plays an important role in increasing the diversity of transcripts encoding MHC molecules (Ishitani and Geraghty 1992) and in modulating intracellular signaling and intercellular interactions through the expression of various isoforms of key cytokines (Bihl et al. 2002; Nishimura et al. 2000), cytokine receptors (Rao et al. 2005; Goodwin et al. 1990; Koskinen et al. 2009), kinases (Jensen and Whitehead 2001) and adaptor proteins (Gray et al. 2010; Ohta et al. 2004; Janssens et al. 2002).

78 Yet, the extent to which changes in isoform usage are a hallmark of immune
79 responses to infection remains largely unexplored at a genome-wide level (Alasoo et
80 al. 2015; Rodrigues et al. 2013). Moreover, we still do not know which RNA
81 processing mechanisms contribute most to the regulation of immune responses, or
82 how these disparate mechanisms are coordinated.
83
84 To address these questions, we investigated genome-wide changes in transcriptome
85 patterns after independent infections with *Listeria monocytogenes* or *Salmonella*
86 *typhimurium* in primary human macrophages. Because of the distinct molecular
87 composition of these two pathogens and the way they interact with host cells, they
88 activate distinct innate immune pathways after infection (Haraga et al. 2008; Pamer
89 2004). Thus, our study design allowed us to evaluate the extent to which changes in
90 isoform usage are pathogen-specific or more generally observed in response to
91 bacterial infection. Furthermore, the large number of individuals in our study
92 allowed us to use natural variation in RNA processing to gain insight into fine-tuned
93 inter-individual regulation of immune responses. Our results provide a
94 comprehensive picture of the role of RNA processing in regulating early innate
95 immune responses to bacterial infection in human antigen-presenting cells.
96
97 **RESULTS**
98
99 Infection with either *Listeria* or *Salmonella* induces dramatic changes in mRNA
100 expression levels. Following 2 hours of infection with each bacteria, we collected
101 RNA-seq data from 60 matched non-infected and infected samples, with an average
102 of 30 million reads sequenced per sample (see Methods; Table S1). The first
103 principal component of the complete gene expression data set clearly separated
104 infected from non-infected samples, and both PC1 and PC2 clustered infected
105 samples by pathogen (i.e. *Listeria* or *Salmonella*; Figure 1A). Accordingly, we
106 observed a large number of differences in gene expression levels between infected
107 and non-infected cells, with 5,809 (39%) and 7,618 (51%) of genes showing
108 evidence for differential gene expression (DGE) after infection with *Listeria* and

109 *Salmonella*, respectively (using DESeq2, FDR ≤ 0.1% and $|\log_2(\text{fold change})| > 0.5$;
110 Figure S1A, Table S2). As expected, the sets of genes that responded to either
111 infection were strongly enriched (FDR ≤ 1.8×10^{-6}) for genes involved in immune-
112 related biological processes such as the regulation of cytokine production,
113 inflammatory responses, or T-cell activation (Table S3).
114
115 In order to uncover changes in isoform usage in response to infection using our
116 RNA-sequencing data, we applied two complementary approaches for analyzing
117 RNA processing. We first measured abundances of full isoforms to gain a holistic
118 perspective of the transcriptome landscape. Second, we used the relative
119 abundances of individual exons within a gene to gain a finer understanding of the
120 specific RNA processing mechanisms likely to be involved in the regulation of
121 immune responses.
122
123 **Pervasive differential isoform usage in response to infection.** We initially
124 sought to assess changes in isoform usage after infection using proportional
125 abundances of the different isoforms encoded by the same gene. To do so, we used
126 the transcripts per million (TPM) values reported by the RSEM software (Li et al.
127 2010) and calculated relative proportions by dividing isoform-level expression by
128 the overall expression level of the gene (i.e., TPM summed across all possible
129 isoforms). We then quantified differential isoform usage (DIU) between conditions
130 for genes with at least two annotated isoforms (*N = 11,353*) using a multivariate
131 generalization of the Welch's t-test that allowed us to test whether, as a group, the
132 proportional abundances of the different isoforms in each gene were significantly
133 different between infected and non-infected cells (Methods). We found that 1,456
134 (13%; after *Listeria* infection) and 2,862 (25%; after *Salmonella* infection) genes
135 showed evidence for significant DIU after infection (FDR ≤ 1%; Figure 1B for an
136 example of an DIU gene, Figure S1B, Table S4). Across all DIU genes, we observed a
137 mean of 10% (± 8% s.d.) and 13% (± 10% s.d.) change in relative isoform usage
138 upon infection with *Listeria* and *Salmonella*, respectively (defined as the maximum
139 change upon infection in relative isoform usage across transcripts of each gene,

140 Figure S1C). Following infection with *Listeria* and *Salmonella*, 6.2% and 10.2%,
141 respectively, of genes with a dominant isoform prior to infection (see methods) switch to
142 using an alternative dominant isoform (Figure S1E).
143
144 DIU genes were significantly enriched for genes involved in immune responses (FDR
145 ≤ 0.01; Table S3), including several cytokines (e.g. *IL1B*, *IL7*, *IL20*), chemokines
146 (*CCL15*), regulators of inflammatory signals (e.g. *ADORA3*, *MAP3K14*) and genes
147 encoding co-stimulatory molecules required for T cell activation and survival (e.g.
148 *CD28* in Figure 1B, *CD80*) (Figure S2). Notably, 86% of genes with DIU upon
149 infection with *Listeria* were also classified as having DIU after infection with
150 *Salmonella*, suggesting that changes in isoform usage are likely to be common across
151 a wide variety of immune triggers. To assess the robustness of our findings, we
152 tested for DIU using isoform-specific expression levels calculated with Kallisto, an
153 alignment-free quantification method (Bray et al. 2016) (see Supplementary
154 Methods). At an FDR of 5%, we observed a 74% (*Listeria*) and 78% (*Salmonella*)
155 agreement with DIU genes identified using RSEM, confirming that identification of
156 DIU genes is largely robust to the method used for isoform quantification.
157
158 Considering the large proportion of genes with significant DIU upon infection, we
159 sought to understand whether these changes arose from a shift in the usage of a
160 dominant isoform or increased isoform diversity within a given gene. To do so, we
161 calculated the Shannon diversity index, which measures the evenness of the isoform
162 usage distribution for each gene before and after infection (low values reflect usage
163 of one or few isoforms; high values reflect either the usage of a more diverse set of
164 isoforms or more equal representation of the same set of isoforms). Δ_{Shannon} thus
165 quantifies the change in isoform diversity after infection (Table S5). The majority of
166 genes (63% in *Listeria* and 68% in *Salmonella*) show an increase in isoform
167 diversity ($\Delta_{\text{Shannon}} > 0$) after infection (Figure S1D), indicating a shift away from
168 usage of the primary (pre-infection) isoform after infection and a general increase in
169 the diversity of transcript species following infection.

170

171 Previously, it had been reported that DGE and DIU generally act independently to
172 shape the transcriptomes of different mammalian tissues (Barbosa-Morais et al.
173 2012). In contrast, we found that DIU genes were significantly enriched for genes
174 with DGE (both up- and down-regulated genes, Fisher's exact test, $P \leq 7.5 \times 10^{-6}$ for
175 both *Listeria* and *Salmonella*) (Figure S3A). Despite such enrichment, a substantial
176 proportion of genes (47% (690 genes) in *Listeria* infected samples and 39% (1,105
177 genes) in *Salmonella* infected samples) with significant changes in isoform usage
178 after infection do not exhibit DGE following infection (Figure 1C). Even after
179 relaxing the FDR threshold for DGE by 100-fold, 685 (*Listeria*) and 1096
180 (*Salmonella*) DIU genes still exhibited no significant DGE. Thus, a considerable
181 fraction of transcriptome changes in response to infection do occur solely at the
182 level of RNA processing, and independently of changes in mean expression levels.

183

184 **Directed shifts in 3' UTR length and alternative splicing following infection.**
185 Though useful in documenting the substantial transcriptome changes upon
186 infection, aggregate isoform levels calculated by RSEM do not distinguish between
187 different types of RNA processing changes. Thus, we next examined changes in five
188 distinct categories of alternative RNA processing, allowing us to zoom in on
189 particular molecular mechanisms that underlie differential isoform usage in
190 response to infection. Specifically, we used human transcript annotations from
191 Ensembl to quantify usage of (1) alternative first exons (AFEs), (2) alternative last
192 exons (ALEs), (3) alternative polyadenylation sites, leading to tandem 3'
193 untranslated regions (TandemUTRs), (4) retained introns (RIs), and (5) skipped
194 exons (SEs). AFEs, ALEs, and TandemUTRs correspond to the alternative usage of
195 terminal exons primarily affecting UTR composition, whereas RIs and SEs
196 correspond to internal splicing events that usually affect the open reading frame.

197

198 For each gene or exon within each RNA processing category, we used the MISO
199 software (Katz et al. 2010) to calculate a "percent spliced in" (PSI or Ψ) value (Table
200 S6), defined as the proportion of transcripts from a gene that contain the "inclusion"

201 isoform (defined as the longer isoform for RIs, SEs, and TandemUTRs, or use of the
202 exon most distal to the gene for AFEs and ALEs). ΔΨ values thus represent the
203 difference between PSI values calculated for the infected versus non-infected
204 samples. Overall, we observed many significant changes in RNA processing ($N \geq$
205 *1,098*) across all categories in both bacteria (significance was defined as Bayes
206 Factor > 5 in at least 10% of individuals and |mean ΔΨ| > 0.05), compared to null
207 expectations derived from measuring changes among pairs of non-infected samples
208 (N=29) (Figure 2A, Table S7). Our criteria for determining significant changes also
209 allows us to choose exons that are more likely to be consistently changing across
210 many individuals; significantly changing exons have lower variance in ΔΨ values
211 across individuals than exons that are not changing after infection (Figure S4). The
212 greatest proportion of changes after infection occurred among retained intron and
213 TandemUTR events. PSI values for 7.3% and 14% of retained introns and 7.6% and
214 16.7% of TandemUTRs significantly changed after infection with *Listeria* or
215 *Salmonella*, respectively. When we considered the set of genes associated with at
216 least one significant change in RNA processing, we observed an over-representation
217 of Gene Ontology categories involved in immune cell processes and the cellular
218 response to a stimulus (Figure 2B, Table S8).
219
220 Genome-wide shifts towards more prevalent usage of inclusion or exclusion
221 isoforms have previously been observed as signatures of cellular stress responses or
222 developmental processes (Sandberg et al. 2008; Mayr and Bartel 2009; Wong et al.
223 2013; Lackford et al. 2014a; Shalgi et al. 2014; Ji et al. 2009). To examine directional
224 shifts in particular RNA processing mechanisms, we used mean ΔΨ values (defined
225 as the mean ΔΨ across all individuals for each gene or exon) and observed a striking
226 global shift towards the usage of upstream polyadenylation sites in tandem 3' UTR
227 regions, indicating pervasive 3' UTR shortening following infection with either
228 *Listeria* or *Salmonella* (Figure 2C; both $P < 2.2\times10^{-16}$ with Mann-Whitney U test;
229 94.4% and 98% of significant TandemUTRs changes in *Listeria* and *Salmonella*).
230 Although less frequent, we also see a general trend towards usage of upstream
231 polyadenylation sites in alternative last exons. Interestingly, we found a striking

232 correlation in the extent to which a given individual has a global shift towards 3'
233 UTR shortening and towards usage of an upstream ALE (Pearson R = 0.83, $P = 4.97 \times$
234 10^{-16} for Listeria and Pearson R = 0.78, $P = 2.65 \times 10^{-13}$ for Salmonella, Figure S6B).
235 These correlations suggest that the changes in ALEs and TandemUTRs are likely
236 being regulated by similar or coordinated mechanisms; rather they are likely
237 regulated through changes in the activities of cleavage and polyadenylation factors
238 (rather than splicing machinery), as suggested by previous reports (Takagaki and
239 Manley 1998; Di Giammartino et al. 2011; Taliaferro et al. 2016). Additionally, we
240 found a substantial increase in the inclusion of skipped exons after infection (both P
241 $< 2.2\times10^{-16}$ with Mann-Whitney U test; 79.8% and 77.3 % of significant SE changes
242 in *Listeria* and *Salmonella*, Figure S5). The consistency of these patterns suggests
243 that a dedicated post-transcriptional regulatory program might underlie genome-
244 wide shifts in RNA processing after bacterial infection.
245
246 Quantifying changes at the terminal ends of transcripts is challenging due to known
247 biases in standard RNA-seq protocols (Wang et al. 2009). Thus, we validated our
248 observation of 3' UTR shortening upon infection by sequencing RNA from 6
249 individuals after infection with *Listeria* and *Salmonella* with a 3'RNA-seq protocol,
250 which specifically captures the 3' most end of transcripts (see Methods). TPM
251 expression values calculated from 3' RNA-seq data highly correlate with TPMs from
252 RNA-seq data, establishing that this method is able to quantitatively measure of the
253 number of transcripts in a cell (R > 0.82 across all conditions, $P < 2.2 \times 10^{-16}$, Figure
254 S6). Meta-gene plots around the polyadenylation sites of core and extended regions
255 of TandemUTRs show a notable increase after infection in sequencing coverage
256 around the upstream polyadenylation site relative to the downstream
257 polyadenylation site, specifically for genes with significantly shorter 3' UTRs upon
258 infection as assessed by the RNA-seq data (Figure 3A) Finally, to look at 3' UTR
259 shortening in specific genes, we calculate Ψ values for TandemUTRs using the
260 3'RNA-seq data (see Supplementary Methods) and find again that genes that are

261 significantly changing 3' UTR usage in the RNA-seq data exhibit a significant shift
262 towards negative ΔΨ values in the 3'RNA-seq data ($P < 2.2 \times 10^{-16}$; Figure 3B).
263
264 **RNA processing changes persist 24 hours after infection.** To evaluate whether
265 the strong global shifts we observed were the result of a sustained immune
266 response to the bacteria rather than a short-lived cellular stress response, we
267 sequenced RNA from a subset of our individuals (*N=6*) after 24 hours (h) of
268 infection with *Listeria* or *Salmonella*. Samples sequenced after 24h were paired with
269 matched non-infected controls cultured for 24h to calculate ΔΨ values for
270 alternative RNA processing categories using MISO (Katz et al. 2010). Across all
271 categories, we found many more significant changes in RNA processing and larger
272 ΔΨ values after infection for 24h than after 2h (Figure S7). These results further
273 support a key role for RNA processing in controlling innate immune responses to
274 infection. For genes or exons that changed significantly after 2h of infection in this
275 set of 6 individuals (see Methods), the majority of changes (67%) remained
276 detectable at 24h, usually with similar magnitude and direction (Figure 4A). The one
277 notable exception is that introns that are preferentially retained at 2h in infected
278 cells tended to be spliced out at 24h. Our results thus indicate that the splicing of
279 alternative retained introns during the course of the immune response to infection
280 is temporally dynamic.
281
282 **Shortening of 3' UTR regions and increased exon inclusion are evolutionarily**
283 **conserved responses to infection in primates.** Since the innate immune response
284 is ancient, one might expect core aspects of this pathway to be evolutionarily
285 conserved among primates. To explore this question, we used high-depth RNA-seq
286 data from human, chimpanzee, and rhesus macaque primary whole blood cells (*N=6*
287 individuals from each species) before and after 4 hours of stimulation with
288 lipopolysaccharide (LPS), the major component of the outer membrane of Gram-
289 negative bacteria. Using an analysis pipeline similar to our analysis of infection after
290 24 hours of infection with *Listeria* or *Salmonella*, we calculated ΔΨ values for

291 alternative RNA processing categories using MISO (Katz et al. 2010) (see
292 Supplementary Methods, Table S9). As with macrophages, we observed consistent
293 strong shifts towards increased exon inclusion and shorter 3' UTRs in human whole
294 blood cells stimulated with LPS. Furthermore, we observed similar trends toward
295 increased exon inclusion and significant 3' UTR shortening in macaques and
296 chimpanzees, supporting a conserved response of RNA processing pathways during
297 innate immune responses in primates (Figure 4B). In addition, these data shows
298 that the shortening of 3' UTRs and increased exon inclusion are not limited to
299 isolated macrophages but also observed as part of the immune response engaged by
300 interacting primary granulocytes and lymphocytes, more closely mimicking *in vivo*
301 cellular responses to infection.
302
303 **Increased exon inclusion is associated with increased gene expression levels.**
304 Since we observed strong connections between overall isoform usage and
305 differential gene expression, we explored the relationship between the occurrence
306 of particular RNA processing changes and the direction of gene expression changes
307 in response to infection. We found that genes with significant differences in skipped
308 exon usage pre- and post-infection (up to 80% of which have increased skipped
309 exon inclusion after infection) were more likely to be up-regulated after infection
310 (T-test, both $P \leq 1\times10^{-4}$ for *Listeria* and *Salmonella*; Figure 5A; Figure S8A). This
311 association remained when gene expression levels were calculated using reads
312 mapping to constitutive exons only (Figure S8A), eliminating concerns about
313 alternative spliced isoforms impacting gene expression estimates. Our observation
314 is consistent with a recent study that reported increased gene expression in tissues
315 with increased inclusion of evolutionarily novel SEs (Merkin et al. 2015). Genes with
316 other types of splicing changes showed no trend in expression changes.
317
318 Genes with significant skipped exon usage were enriched for Gene Ontology
319 categories such as "response to stimulus," and also for "RNA processing" and "RNA
320 stability" categories (Figure S9A). Included within these latter categories are several
321 members of two major splicing factor families, SR proteins and hnRNPs, which

322 showed increased inclusion of skipped exons and increased gene expression after
323 infection (Figure S9B). The SR protein and hnRNP families are known to function in
324 complex auto- and cross-regulatory networks (Huelga et al. 2012; Pandit et al.
325 2013), often antagonizing one another's effects on splicing (House and Lynch 2008;
326 Wang and Burge 2008; Busch and Hertel 2012). Consistent with the slightly higher
327 up-regulation of members of the hnRNP family, we observed a consistent
328 enrichment for intronic splicing silencers in upstream intronic regions around
329 significantly excluded skipped exons (Figure S9C). These elements are often bound
330 by hnRNPs to promote exclusion of a cassette exon (Wang and Burge 2008))
331
332 **Variation across individuals provides insight into putative trans-regulatory**
333 **factors.** A unique feature of our study design is our sampling of 60 individuals after
334 infection with both *Listeria* and *Salmonella*. By taking advantage of natural variation
335 in the regulation of RNA processing to infection, we aimed to gain further insight
336 into the connections between RNA processing and changes in gene expression levels
337 in response to infection. For each gene, we calculated the correlation between the
338 inter-individual variation in RNA processing changes ($\Delta\Psi$) and the fold changes in
339 gene expression levels upon infection. For most categories, we observed shifts in the
340 distribution of correlations between RNA processing and gene expression levels
341 relative to permuted controls (Figure S8B), with skipped exons and TandemUTRs
342 showing the most consistent patterns (Kolmogorov-Smirnov test, $P \leq 0.005$; Figure
343 5B). Increased skipped exon inclusion correlates with increased gene expression of
344 the gene across individuals in 69% of the genes with significant skipped exons. In
345 addition, preferential expression of shorter alternative 3' UTR isoforms tends to be
346 correlated with increased up-regulation of the associated genes in response to
347 infection. Our findings thus suggest that RNA processing changes may directly
348 impact gene expression levels, or at least are commonly regulated with changes in
349 transcription or mRNA stability.
350
351 Substantial inter-individual variation in the genome-wide average RNA processing
352 patterns also correlated strongly with average gene expression changes upon

353 infection, particularly for changes in 3' UTR usage. That is, individuals who exhibited
354 more skipped exon inclusion or 3' UTR shortening also tended to exhibit larger
355 global shifts towards up-regulation of gene expression levels upon infection (Figure
356 S10B).
357
358 Next, we sought to exploit our relatively large sample size to identify candidate
359 *trans*-factors impacting the amount of skipped exon and TandemUTR changes
360 observed across individuals. Specifically, we examined the relationship between
361 mean changes in exon inclusion and fold change in expression for all expressed
362 genes, across the 60 individuals. When we focus on proteins with known RNA
363 binding functions or domains – hypothesizing that these factors are more likely to
364 regulate post-transcriptional mechanisms – we find many significant correlations
365 (FDR ≤ 1%) for known regulators of the corresponding RNA processing category
366 (Figure S11). For instance, genes whose changes in expression correlated with
367 individual-specific mean 3' UTR shortening included several factors previously
368 implicated in regulating polyadenylation site usage (such as cleavage and
369 polyadenylation factors (Zheng and Tian 2014), hnRNP H proteins (Katz et al. 2010),
370 and hnRNP F (Veraldi et al. 2001); Figure S11A). Additionally, many known
371 regulators of alternative splicing – including a number of SR proteins and hnRNPs –
372 have increased expression levels in individuals with larger extents of skipped exon
373 inclusion (Figure S11B).
374
375 **3' UTR shortening as a means to evade repression by immune-related miRNAs.**
376 The largest global shift observed in alternative isoform abundance was for 3' UTR
377 shortening, where as many as 98% of significantly changing TandemUTRs shifted
378 towards usage of an upstream polyA site post-infection. Previously, global 3' UTR
379 shortening has been associated with proliferating cells, particularly in the context of
380 cellular transitions in development (Sandberg et al. 2008), cell differentiation
381 (Lackford et al. 2014b), cancerous (Mayr and Bartel 2009) states, or global 3' UTR
382 lengthening in embryonic development (Ji et al. 2009). However, macrophages do
383 not proliferate, which we confirmed with a BrdU labeling assay in both resting and

384 infected conditions (Figure S12). This result indicates that the pervasive 3' UTR
385 shortening observed in response to infection is due to an active cellular process that
386 is independent of cell division and might be mechanistically distinct from that
387 leading to 3' UTR shortening in proliferating cells.
388
389 Previous studies in proliferating cells postulated that 3' UTR shortening can act as a
390 way to evade regulation by microRNAs (miRNAs), since crucial miRNA target sites
391 are most often found in 3' UTR regions (Sandberg et al. 2008). To evaluate this
392 hypothesis we performed small-RNA sequencing in 6 individuals after 2h and 24h of
393 infection with *Listeria* and *Salmonella*. When focusing specifically on miRNAs
394 expressed in macrophages (Table S10), we found that the extended UTR regions of
395 infection-sensitive 3' UTRs have a significantly higher density of miRNA target sites
396 compared to TandemUTRs that do not change in response to infection (Figure 6A).
397 This increased density of miRNA target sites was restricted to the extension region,
398 which is subject to shortening after infection: no difference in the density of target
399 sites was observed in the common "core" 3' UTR regions of the same genes (Figure
400 S13).
401
402 Next, we tested if the increased density of miRNA target sites was driven by the
403 enrichment of target sites for particular miRNAs expressed in macrophages. For
404 each miRNA that was expressed in either non-infected or infected macrophages, we
405 calculated an enrichment score assessing whether the target sites of that miRNA
406 were significantly enriched in the extended region of significantly shortened 3' UTRs
407 (with a background distribution matched for sequence composition; Figure S14; see
408 Supplemental Methods). We found 15 miRNAs with significantly enriched target
409 sites (FDR ≤ 10% and enrichment ≥ 1.5 fold) in either the *Listeria* or *Salmonella*
410 conditions, with 6 miRNAs over-represented in both bacterial conditions (Figure
411 6B). Interestingly, of the miRNAs with the highest enrichment after infection with
412 either *Listeria* or *Salmonella*, two (miR-146b and miR-125a) have previously been
413 shown to be important regulators of the innate immune response (Taganov et al.
414 2006; Perry et al. 2009; Boldin and Baltimore 2012; Kim et al. 2012; Banerjee et al.

415 2013). Accordingly, we found that 4 of the miRNAs with the highest enrichment
416 after infection (miR-125a, miR146b, miR-3661, and miR-151b) are all up-regulated
417 following infection, and strongly so after 24h of infection (Figure 6B). In the
418 majority of cases, greater 3' UTR shortening was associated with a stronger increase
419 in gene expression across individuals, suggesting that shifts towards shorter 3' UTRs
420 after infection allows these transcripts to escape from repression by specific
421 immune-induced miRNAs.
422
423 **DISCUSSION**
424
425 Taken together, our results provide strong evidence that RNA processing plays a key
426 role in the regulation of innate immune responses to infection. Despite known
427 differences in the regulatory pathways elicited in macrophages by *Listeria* and
428 *Salmonella*, our data revealed striking similarities in the overall patterns of RNA
429 processing induced in response to both pathogens. Given the strong overlaps, we
430 chose throughout this study to focus on consistent patterns across the two bacteria.
431
432 Though genes that have differential isoform usage in response to infection are more
433 likely to show changes in gene expression, we found that as many as 47% of genes
434 showing differential isoform usage have no evidence for differences in gene
435 expression upon infection. This observation suggests that a considerable proportion
436 of genes are regulated predominantly by post-transcriptional mechanisms, with
437 minimal changes in transcriptional regulation. Differential isoform usage is coupled
438 to a prominent increase in the diversity of isoforms following infection. Intriguingly,
439 genes showing the strongest increases in diversity upon infection were strongly
440 enriched among down-regulated genes (Figure S3B). This observation raises the
441 possibility that the increased isoform diversity could reflect a shift toward less
442 stable isoforms, e.g., those targeted by nonsense-mediated decay (NMD), thus
443 reducing transcript levels (Lewis et al. 2003; Green et al. 2003).
444

445 Upon infection of human macrophages with either *Listeria* or *Salmonella*, we
446 observed substantial shifts towards increased skipped exon inclusion and
447 shortening of 3' UTRs. These RNA processing patterns remained prominent when
448 interrogated in human whole blood after an alternative immune stimulus (LPS),
449 despite the fact the number of significant RNA processing changes in whole blood
450 was generally smaller than that observed in purified macrophages infected with live
451 bacteria. This reduced effect is likely explained by the fact that in whole blood, we
452 are interrogating a very heterogeneous cell population within which only a fraction
453 (~3-6%) of the cell types are actually responding to LPS stimulation, such as
454 monocytes/macrophages (Zarember and Godowski 2002). Additionally,
455 transcriptional changes induced by live bacteria such as *Listeria* or *Salmonella*,
456 which concomitantly activates multiple innate immune pathways (Haraga et al.
457 2008; Pamer 2004), are grander than transcriptional changes that can induced by a
458 single purified ligand, such as LPS, which activates primarily the TLR4 pathway
459 (Poltorak et al. 1998). Despite this reduced statistical power, we still observed
460 conserved RNA processing signatures of immune stimulation through the primate
461 lineage, supporting the likely functional importance of these cellular responses and
462 the ubiquity of RNA processing changes after immune stimulation across evolution.
463
464 The most prominent hallmark of RNA processing changes after infection is a global
465 shortening of 3' UTRs. Interestingly, this effect resembles the global 3' UTR
466 shortening seen in proliferating activated T cells and transformed cells (Sandberg et
467 al. 2008) (Mayr and Bartel 2009) (Lackford et al. 2014b). Given that both T-cell and
468 macrophage activation result in the activation of shared signaling cascades (e.g., c-
469 Jun N-terminal kinase (JNK) – a key regulator of apoptosis – and nuclear factor κ-B
470 (NF-κB) activation), it is possible that, at least to some extent, 3' UTR shortening
471 observed in T-cells and macrophages stems from the activation of these shared
472 pathways. Previous studies hypothesized that 3' UTR shortening allows mRNAs to
473 escape regulation by dynamically changing miRNAs, suggesting that macrophages
474 may co-opt generally used mechanisms for the same purpose. (Sandberg et al. 2008;

475 Mayr and Bartel 2009). This shift towards shorter 3' UTRs could result from
476 increased miRNA-dependent degradation of transcripts with longer 3' UTRs post-
477 infection. However, genes that shift towards shorter 3' UTRs were more highly
478 expressed post-infection, making this explanation unlikely. Furthermore, the
479 increase in overall miRNA target site density is reminiscent of a previous
480 observation that genes with regulated 3' UTR usage across tissues have more target
481 sites for ubiquitously expressed miRNAs in their distal 3' UTRs (Lianoglou et al.
482 2013). However, in contrast to results across tissues, we observe that the target
483 sites in our distal 3' UTR regions are directly related to miRNAs whose expression
484 specifically changes after infection.
485
486 Specifically, our data support previous hypotheses and find evidence for that 3' UTR
487 shortening in macrophages is associated with the loss of target sites for a subset of
488 immune-regulated miRNAs, including miR-146b, miR-125a, and miR-151b (Figure
489 6B). These miRNAs target the extended 3' UTR regions of several critical activators
490 of the innate immune response – including the *IRF5* transcription factor (Lawrence
491 and Natoli 2011) and the MAP kinases *MAPKAP1* and *MAP2K4* (Arthur and Ley
492 2013) – all of which shift to usage of shorter 3' UTRs after infection. It is tempting to
493 speculate that without such 3' UTR shortening, the binding of one or more of
494 miRNAs to the 3' UTR region of these genes would compromise their up-regulation
495 and the subsequent activation of downstream immune defense pathways. Given that
496 many miRNAs are involved in either (or both) mRNA degradation and translational
497 efficiency, we cannot know for sure which of these processes is prevented by the 3'
498 UTR shortening of these genes.
499
500 The convergence towards similar isoform outcomes across many disparate genes
501 suggests the activation of factors acting in *trans* to drive global shifts towards
502 inclusion of cassette exons or usage of upstream proximal polyadenyalation sites.
503 Taking advantage of our relatively large sample size, we were able to identify
504 candidate *trans*-factors whose up-regulation upon infection might have widespread
505 impacts on RNA processing patterns, including some known regulators of

506 alternative splicing or 3'end processing (Figure S11). Sets of RNA binding factors
507 likely act in combination to influence final transcriptome states (Brooks et al. 2015).
508 For instance, a general up-regulation of splicing machinery following infection
509 (Munding et al. 2013), allowing the cell to recognize and use additional splice sites,
510 might contribute to increased exon inclusion and greater isoform diversity observed
511 following infection. Members of both the hnRNP and SR protein splicing factor
512 families show up-regulation of their overall gene expression levels (Figure S9B),
513 likely contributing to specific instances of exon inclusion as well as exclusion.
514 Correspondingly, changes in the regulation of many canonical cleavage and
515 polyadenylation factors were tied to individual-specific shifts in 3' UTR shortening.
516 The significant correlation between global shifts in ALE usage and TandemUTRs
517 across individuals further support the notion that cleavage and poladenylation
518 pathways are regulating the changing 3' UTR landscape upon infection (Figure
519 S10A). Intriguingly, fold changes in hnRNP H1 gene expression have high
520 correlations with both skipped exon inclusion and 3' UTR shortening, consistent
521 with its known splicing function and suggesting that this factor may play multiple
522 roles in shaping the transcriptome in response to bacterial infection.
523
524 An alternative mechanism that has been proposed for the global regulation of 3'
525 UTR shortening in T-cell activation and neuronal differentiation is a phenomenon
526 called *telescripting*. This is a phenomenon by which moderately lower U1 snRNA
527 levels relative to global increases in nascent mRNA production restrict U1's
528 secondary role in inhibiting premature cleavage and polyadenylation (Berg et al.
529 2012). While we did not directly measure mRNA levels, we observe a moderate but
530 significant increase in total RNA concentration after 2 hours of infection that is
531 consistent with the increase in nascent RNA observed by Berg et al. (Berg et al.
532 2012) (across 60 samples, paired t-test; P=0.006 for Listeria and $P=4.57 \times 10^{-6}$ for
533 Salmonella), combined with no changes in the levels of U1 snRNA (relative to 5S
534 rRNA, Supplemental Methods, Figure S15). Thus it is possible that a delayed
535 response of U1 snRNA could promote the usage of upstream polyadenylation sites

536 in both TandemUTRs and ALEs. Interestingly, Berg et al. also observe increased up-
537 regulation of individual internal exons upon moderate U1 knockdown in neurons
538 (Berg et al. 2012), which is consistent with our observation of increased skipped
539 exon inclusion.
540
541 Substantial inter-individual variation in the genome-wide average RNA processing
542 patterns also correlated strongly with average gene expression changes upon
543 infection, particularly for changes in 3' UTRs and skipped exons. That is, individuals
544 who exhibited more skipped exon inclusion or usage of upstream polyadenylation
545 sites also tended to exhibit larger global shifts towards up-regulation of gene
546 expression levels upon infection (Figure S10B). Though these patterns might result
547 from stochastic variation in levels of one or several *trans*-factors, they are also likely
548 to be influenced by genetic differences among individuals. It will be interesting to
549 ask whether global isoform differences might potentially be reflective of variation in
550 an individual's susceptibility to infection.
551
552 **Materials and Methods**
553
554 Complete details of the experimental and statistical procedures can be found in SI
555 Materials and Methods. Briefly, blood samples from 60 healthy donors were
556 obtained from Indiana Blood Center with informed consent and ethics approval
557 from the Research Ethics Board at the CHU Sainte-Justine (protocol #4022). All
558 individuals recruited in this study were healthy males between the ages of 18 and
559 55 y old. Blood mononuclear cells from each donor were isolated by Ficoll-Paque
560 centrifugation and blood monocytes were purified from peripheral blood
561 mononuclear cells (PBMCs) by positive selection with magnetic CD14 MicroBeads
562 (Miltenyi Biotec). In order to derive macrophages, monocytes were then cultured
563 for 7 days in RPMI-1640 (Fisher) supplemented with 10% heat-inactivated FBS
564 (FBS premium, US origin, Wisent), L-glutamine (Fisher) and M-CSF (20ng/mL; R&D
565 systems). After validating the differentiation/activation status of the monocyte-
566 derived macrophages we infected them at a multiplicity of infection (MOI) of 10:1

567 for *Salmonella typhimurium* and an MOI of 5:1 for *Listeria monocytogenes* for 2- and
568 24-hours. For primate comparisons, whole blood was drawn from 6 healthy adult
569 humans (CHU Sainte-Justine), 6 common chimpanzees, (Texas Biomedical Research
570 Institute), and 6 rhesus macaques (Yerkes Regional Primate Center). Human
571 samples were acquired with informed consent and ethics approval from the
572 Research Ethics Board (CHU Sainte-Justine, #3557). Non-human primate samples
573 were acquired in accordance with individual institutional IACUCC requirements. For
574 all species, 1ml of blood was drawn into a media-containing tube (Trueculture tube,
575 Myriad, US) spiked with ultrapure LPS (Invitrogen, USA) or endotoxin-free water
576 (control). Samples were stimulated with 1ug/ml LPS, at 37C for 4 hours before total
577 blood leukocytes were isolated and RNA collected. Genome-wide gene expression
578 profiles of untreated and infected/treated samples were obtained by RNA-
579 sequencing for both mRNA transcripts and small RNAs. After a series of quality
580 checks (SI Materials and Methods), mRNA transcript abundances were estimated
581 using RSEM (Li and Dewey 2011) and Kallisto (Bray et al. 2016) and microRNA
582 expression estimates were obtained as previously described(Siddle et al. 2014). To
583 detect genes with differential isoform usage between two groups of non-infected
584 and infected samples we used a multivariate generalization of the Welch's t-test.
585 Shannon entropy H_{sh} (also known as Shannon index) was applied to measure the
586 diversity of isoforms for each target gene before and after infection. Changes across
587 individual RNA processing events were quantified using the MISO software package
588 (v0.4.9) (Katz et al. 2010) using default settings and hg19 version 1 annotations.
589 Events were considered to be significantly altered post-infection if at least 10% (n
590 >= 6) of individuals had a BF >= 5 and the |mean $\Delta\Psi$| ≥ 0.05 (Table S6). To conduct a
591 targeting sequencing of 3' ends of transcripts, We used Smart-3SEQ (Foley et al,
592 manuscript in preparation), a modified version of the 3SEQ method (Beck et al.
593 2010) . We used a custom gene ontology script to test for enrichment of functional
594 annotations among genes that significantly changed isoform usage in response to
595 infection (SI Materials and Methods). All predicted miRNA target sites within
596 annotated TandemUTR regions were obtained using TargetScan (v6.2) (Friedman et
597 al. 2009).

598

599 **Data Access**

600

601 Data generated in this study have been submitted to the NCBI Gene Expression
602 Omnibus (GEO; http://www.ncbi.hlm.nih.gov/geo/) under the accession number
603 GSE73765, which comprises of the mRNA-seq data (GSE73502) and small RNA-seq
604 data (GSE73478).

605

606

607 **Acknowledgements**

608

609 We thank P Freese for a categorized list of RNA binding proteins, G McVicker for an
610 initial script to perform iterative gene ontology analyses and P Sudmant for help
611 parsing primate transcript annotations. We thank Y Katz, JM Taliaferro, P Sudmant, J
612 Tung, and members of the Barreiro and Burge labs for helpful discussions and
613 comments on the manuscript. This work was supported by grants from the elife
614 senio (232519), the Human Frontiers Science Program (CDA-00025/2012) and the
615 Canada Research Chairs Program (950-228993) (to L.B.B). We thank Calcul Québec
616 and Compute Canada for managing and providing access to the supercomputer
617 Briaree from the University of Montreal, used to do many computations reported in
618 the manuscript. Additional computational resources were performed on an MIT
619 computational cluster supported by the National Science Foundation (Grant No.
620 0821391). A.A.P. was supported by a Jane Coffin Childs postdoctoral fellowship. G. B.
621 was supported by a postdoctoral fellowship from the Fonds de la Recherche en
622 Santé du Québec.

623

624

625 **References**
626

627 Alasoo K, Estrada FM, Hale C, Gordon S, Powrie F. 2015. Transcriptional profiling of
628 macrophages derived from monocytes and iPS cells identifies a conserved
629 response to LPS and novel alternative transcription. *bioRxiv*.

630 Arthur JSC, Ley SC. 2013. Mitogen-activated protein kinases in innate immunity.
631 *Nature Reviews Immunology* **13**: 679–692.

632 Banerjee S, Cui H, Xie N, Tan Z, Yang S, Icyuz M, Thannickal VJ, Abraham E, Liu G.
633 2013. miR-125a-5p Regulates Differential Activation of Macrophages and
634 Inflammation. *Journal of Biological Chemistry* **288**: 35428–35436.

635 Barbosa-Morais NL, Irimia M, Pan Q, Xiong HY, Gueroussov S, Lee LJ, Slobodeniuc V,
636 Kutter C, Watt S, Çolak R, et al. 2012. The evolutionary landscape of alternative
637 splicing in vertebrate species. *Science* **338**: 1587–1593.

638 Beck AH, Weng Z, Witten DM, Zhu S, Foley JW, Lacroute P, Smith CL, Tibshirani R,
639 van de Rijn M, Sidow A, et al. 2010. 3′-End Sequencing for Expression
640 Quantification (3SEQ) from Archival Tumor Samples ed. I.O.L. Ng. *PLoS One* **5**:
641 e8768.

642 Berg MG, Singh LN, Younis I, Liu Q, Pinto AM, Kaida D, Zhang Z, Cho S, Sherrill-Mix S,
643 Wan L, et al. 2012. U1 snRNP Determines mRNA Length and Regulates Isoform
644 Expression. *Cell* **150**: 53–64.

645 Bihl MP, Heinimann K, Rudiger JJ, Eickelberg O, Perruchoud AP, Tamm M, Roth M.
646 2002. Identification of a novel IL-6 isoform binding to the endogenous IL-6
647 receptor. *American journal of respiratory cell and molecular biology* **27**: 48–56.

648 Boldin MP, Baltimore D. 2012. MicroRNAs, new effectors and regulators of NF-κB.
649 *Immunological Reviews* **246**: 205–220.

650 Bray NL, Pimentel H, Melsted P, Pachter L. 2016. Near-optimal probabilistic RNA-seq
651 quantification. *Nature Biotechnology*.

652 Brooks AN, Duff MO, May G, Yang L, Bolisetty M, Landolin J, Wan K, Sandler J,
653 Celniker SE, Graveley BR, et al. 2015. Regulation of alternative splicing in
654 Drosophila by 56 RNA binding proteins. *Genome Research* gr.192518.115.

655 Busch A, Hertel KJ. 2012. Evolution of SR protein and hnRNP splicing regulatory
656 factors. *WIREs RNA* **3**: 1–12.

657 Di Giammartino DC, Nishida K, Manley JL. 2011. Mechanisms and Consequences of
658 Alternative Polyadenylation. *Molecular Cell* **43**: 853–866.

659 Friedman RC, Farh KK-H, Burge CB, Bartel DP. 2009. Most mammalian mRNAs are

660 conserved targets of microRNAs. *Genome Research* **19**: 92–105.

661 Goodwin RG, Friend D, Ziegler SF, Jerzy R, Falk BA, Gimpel S, Cosman D, Dower SK,
662 March CJ, Namen AE, et al. 1990. Cloning of the human and murine interleukin-7
663 receptors: demonstration of a soluble form and homology to a new receptor
664 superfamily. *Cell* **60**: 941–951.

665 Gray P, Michelsen KS, Sirois CM, Lowe E, Shimada K, Crother TR, Chen S, Brikos C,
666 Bulut Y, Latz E, et al. 2010. Identification of a novel human MD-2 splice variant
667 that negatively regulates Lipopolysaccharide-induced TLR4 signaling. *The*
668 *Journal of Immunology* **184**: 6359–6366.

669 Green RE, Lewis BP, Hillman RT, Blanchette M, Lareau LF, Garnett AT, Rio DC,
670 Brenner SE. 2003. Widespread predicted nonsense-mediated mRNA decay of
671 alternatively-spliced transcripts of human normal and disease genes.
672 *Bioinformatics* **19**: i118–i121.

673 Haraga A, Ohlson MB, Miller SI. 2008. Salmonellae interplay with host cells. *Nature*
674 *Reviews Microbiology* **6**: 53–66.

675 House AE, Lynch KW. 2008. Regulation of Alternative Splicing: More than Just the
676 ABCs. *Journal of Biological Chemistry* **283**: 1217–1221.

677 Huang Q, Liu D, Majewski P, Schulte LC, Korn JM, Young RA, Lander ES, Hacohen N.
678 2001. The Plasticity of Dendritic Cell Responses to Pathogens and Their
679 Components. *Science* **294**: 870–875.

680 Huelga SC, Vu AQ, Arnold JD, Liang TY, Liu PP, Yan BY, Donohue JP, Shiue L, Hoon S,
681 Brenner S, et al. 2012. Integrative Genome-wide Analysis Reveals Cooperative
682 Regulation of Alternative Splicing by hnRNP Proteins. *Cell Reports* **1**: 167–178.

683 Ishitani A, Geraghty DE. 1992. Alternative splicing of HLA-G transcripts yields
684 proteins with primary structures resembling both class I and class II antigens.
685 *Proceedings of the National Academy of Sciences* **89**: 3947–3951.

686 Janssens S, Burns K, Tschopp J, Beyaert R. 2002. Regulation of interleukin-1-and
687 lipopolysaccharide-induced NF-κB activation by alternative splicing of MyD88.
688 *Current Biology* **12**: 467–471.

689 Jensen LE, Whitehead AS. 2001. IRAK1b, a novel alternative splice variant of
690 interleukin-1 receptor-associated kinase (IRAK), mediates interleukin-1
691 signaling and has prolonged stability. *Journal of Biological Chemistry* **276**:
692 29037–29044.

693 Ji Z, Lee JY, Pan Z, Jiang B, Bin Tian. 2009. Progressive lengthening of 3' untranslated
694 regions of mRNAs by alternative polyadenylation during mouse embryonic
695 development ed. J. Valcarcel. *PNAS* **106**: 7028–7033.

696 Katz Y, Wang ET, Airoldi EM, Burge CB. 2010. Analysis and design of RNA
697 sequencing experiments for identifying isoform regulation. *Nat Meth* **7**: 1009–
698 1015.
699 http://www.nature.com.proxy.uchicago.edu/nmeth/journal/v7/n12/pdf/nmet
700 h.1528.pdf.

701 Kawai T, Akira S. 2010. The role of pattern-recognition receptors in innate
702 immunity: update on Toll-like receptors. *Nat Immunol* **11**: 373–384.

703 Kim SW, Ramasamy K, Bouamar H. 2012. MicroRNAs miR-125a and miR-125b
704 constitutively activate the NF-κB pathway by targeting the tumor necrosis factor
705 alpha-induced protein 3 (TNFAIP3, A20).

706 Koskinen LL, Einarsdottir E, Dukes E, Heap GA, Dubois P, Korponay-Szabo IR,
707 Kaukinen K, Kurppa K, Ziberna F, Vatta S, et al. 2009. Association study of the
708 IL18RAP locus in three European populations with coeliac disease. *Hum Mol*
709 *Genet* **18**: 1148–1155.

710 Lackford B, Yao C, Charles GM, Weng L, Zheng X, Choi EA, Xie X, Wan J, Xing Y,
711 Freudenberg JM, et al. 2014a. Fip1 regulates mRNA alternative polyadenylation
712 to promote stem cell self-renewal. *The EMBO Journal* **33**: 878–889.

713 Lackford B, Yao C, Charles GM, Weng L, Zheng X, Choi EA, Xie X, Wan J, Xing Y,
714 Freudenberg JM, et al. 2014b. Fip1 regulates mRNA alternative polyadenylation
715 to promote stem cell self-renewal. *The EMBO Journal* **33**: 878–889.

716 Lawrence T, Natoli G. 2011. Transcriptional regulation of macrophage polarization:
717 enabling diversity with identity. *Nature Reviews Immunology* **11**: 750–761.

718 Lewis BP, Green RE, Brenner SE. 2003. Evidence for the widespread coupling of
719 alternative splicing and nonsense-mediated mRNA decay in humans. *PNAS* **100**:
720 189–192.

721 Li B, Dewey CN. 2011. RSEM: accurate transcript quantification from RNA-Seq data
722 with or without a reference genome. *BMC Bioinformatics* **12**: 323.

723 Li B, Ruotti V, Stewart RM, Thomson JA, Dewey CN. 2010. RNA-Seq gene expression
724 estimation with read mapping uncertainty. *Bioinformatics* **26**: 493–500.

725 Lianoglou S, Garg V, Yang JL, Leslie CS, Mayr C. 2013. Ubiquitously transcribed genes
726 use alternative polyadenylation to achieve tissue-specific expression. *Genes &*
727 *Development* **27**: 2380–2396.

728 Lynch KW. 2004. Consequences of regulated pre-mRNA splicing in the immune
729 system. *Nature Reviews Immunology* **4**: 931–940.

730 Martinez NM, Lynch KW. 2013. Control of alternative splicing in immune responses:

731 many regulators, many predictions, much still to learn. *Immunological Reviews*
732 **253**: 216–236.

733 Mayr C, Bartel DP. 2009. Widespread Shortening of 3´UTRs by Alternative Cleavage
734 and Polyadenylation Activates Oncogenes in Cancer Cells. *Cell* **138**: 673–684.

735 Medzhitov R, Horng T. 2009. Transcriptional control of the inflammatory response.
736 *Nature Reviews Immunology* **9**: 692–703.

737 Medzhitov R, Janeway CA Jr. 1998. Innate immune recognition and control of
738 adaptive immune responses. *Seminars in Immunology* **10**: 351–353.

739 Merkin JJ, Chen P, Alexis MS, Hautaniemi SK. 2015. Origins and impacts of new
740 mammalian exons. *Cell Reports* **10**: 1992–2005.

741 Munding EM, Shiue L, Katzman S, Donohue JP, Ares M Jr. 2013. Competition between
742 Pre-mRNAs for the Splicing MachineryDrives Global Regulation of Splicing.
743 *Molecular Cell* **51**: 338–348.

744 Nishimura H, Yajima T, Naiki Y, Tsunobuchi H, Umemura M, Itano K, Matsuguchi T,
745 Suzuki M, Ohashi PS, Yoshikai Y. 2000. Differential roles of interleukin 15 mRNA
746 isoforms generated by alternative splicing in immune responses in vivo. *The*
747 *Journal of experimental medicine* **191**: 157–170.

748 Ohta S, Bahrun U, Tanaka M, Kimoto M. 2004. Identification of a novel isoform of
749 MD-2 that downregulates lipopolysaccharide signaling. *Biochem Biophys Res*
750 *Commun* **323**: 1103–1108.

751 O'Connor BP, Danhorn T, De Arras L, Flatley BR, Marcus RA, Farias-Hesson E, Leach
752 SM, Alper S. 2015. Regulation of Toll-like Receptor Signaling by the SF3a mRNA
753 Splicing Complex ed. X. Lin. *PLoS Genet* **11**: e1004932.

754 Pamer EG. 2004. Immune responses to Listeria monocytogenes. *Nature Reviews*
755 *Immunology* **4**: 812–823.

756 Pandit S, Zhou Y, Shiue L, Coutinho-Mansfield G, Li H, Qiu J, Huang J, Yeo GW, Ares M,
757 Fu X-D. 2013. Genome-wide analysis reveals SR protein cooperation and
758 competition in regulated splicing. *Molecular Cell* **50**: 223–235.

759 Perry MM, Williams AE, Tsitsiou E, Larner-Svensson HM, Lindsay MA. 2009.
760 Divergent intracellular pathways regulate interleukin-1β-induced miR-146a and
761 miR-146b expression and chemokine release in human alveolar epithelial cells.
762 *FEBS Letters* **583**: 3349–3355.

763 Poltorak A, He X, Smirnova I, Liu M-Y, Van Huffel C, Du X, Birdwell D, Alejos E, Silva
764 M, Galanos C, et al. 1998. Defective LPS Signaling in C3H/HeJ and C57BL/10ScCr
765 Mice: Mutations in Tlr4 Gene. *Science* **282**: 2085–2088.

766 Rao N, Nguyen S, Ngo K, Fung-Leung W-P. 2005. A novel splice variant of
767 interleukin-1 receptor (IL-1R)-associated kinase 1 plays a negative regulatory
768 role in Toll/IL-1R-induced inflammatory signaling. *Molecular and Cellular*
769 *Biology* **25**: 6521–6532.

770 Rodrigues R, Grosso AR, Moita L. 2013. Genome-wide analysis of alternative splicing
771 during dendritic cell response to a bacterial challenge. *PLoS One*.

772 Sandberg R, Neilson JR, Sarma A, Sharp PA, Burge CB. 2008. Proliferating Cells
773 Express mRNAs with Shortened 3' Untranslated Regions and Fewer MicroRNA
774 Target Sites. *Science* **320**: 1643–1647.

775 Shalgi R, Hurt JA, Lindquist S, Burge CB. 2014. Widespread inhibition of
776 posttranscriptional splicing shapes the cellular transcriptome following heat
777 shock. *Cell Reports* **7**: 1362–1370.

778 Siddle KJ, Deschamps M, Tailleux L. 2014. A genomic portrait of the genetic
779 architecture and regulatory impact of microRNA expression in response to
780 infection. *Genome Research*.

781 Smale ST. 2010. Selective Transcription in Response to an Inflammatory Stimulus.
782 *Cell* **140**: 833–844.

783 Taganov KD, Boldin MP, Chang KJ. 2006. NF-κB-dependent induction of microRNA
784 miR-146, an inhibitor targeted to signaling proteins of innate immune
785 responses.

786 Takagaki Y, Manley JL. 1998. Levels of Polyadenylation Factor CstF-64 Control IgM
787 Heavy Chain mRNA Accumulation and Other Events Associated with B Cell
788 Differentiation. *Molecular Cell* **2**: 761–771.

789 Taliaferro JM, Vidaki M, Oliveira R, Olson S, Zhan L, Saxena T, Wang ET, Graveley BR,
790 Gertler FB, Swanson MS, et al. 2016. Distal Alternative Last Exons Localize
791 mRNAs to Neural Projections. *Molecular Cell* **61**: 821–833.

792 Veraldi KL, Arhin GK, Martincic K, Chung-Ganster LH, Wilusz J, Milcarek C. 2001.
793 hnRNP F Influences Binding of a 64-Kilodalton Subunit of Cleavage Stimulation
794 Factor to mRNA Precursors in Mouse B Cells. *Molecular and Cellular Biology* **21**:
795 1228–1238.

796 Wang Z, Burge CB. 2008. Splicing regulation: From a parts list of regulatory
797 elements to an integrated splicing code. *RNA* **14**: 802–813.

798 Wang Z, Gerstein M, Snyder M. 2009. RNA-Seq: a revolutionary tool for
799 transcriptomics. *Nat Rev Genet* **10**: 57–63.

800 Wells CA, Chalk AM, Forrest A, Taylor D, Waddell N, Schroder K, Himes SR, Faulkner

801 G, Lo S, Kasukawa T, et al. 2006. Alternate transcription of the Toll-like receptor
802 signaling cascade. *Genome Biology* **7**: R10.

803 Wong JJL, Ritchie W, Ebner OA, Selbach M, Wong JWH, Huang Y, Gao D, Pinello N,
804 Gonzalez M, Baidya K, et al. 2013. Orchestrated Intron Retention Regulates
805 Normal Granulocyte Differentiation. *Cell* **154**: 583–595.

806 Zarember KA, Godowski PJ. 2002. Tissue Expression of Human Toll-Like Receptors
807 and Differential Regulation of Toll-Like Receptor mRNAs in Leukocytes in
808 Response to Microbes, Their Products, and Cytokines. *The Journal of*
809 *Immunology* **168**: 554–561.

810 Zheng D, Tian B. 2014. RNA-binding proteins in regulation of alternative cleavage
811 and polyadenylation. In *Systems Biology of RNA Binding Proteins*, pp. 97–127,
812 Springer.

813

814

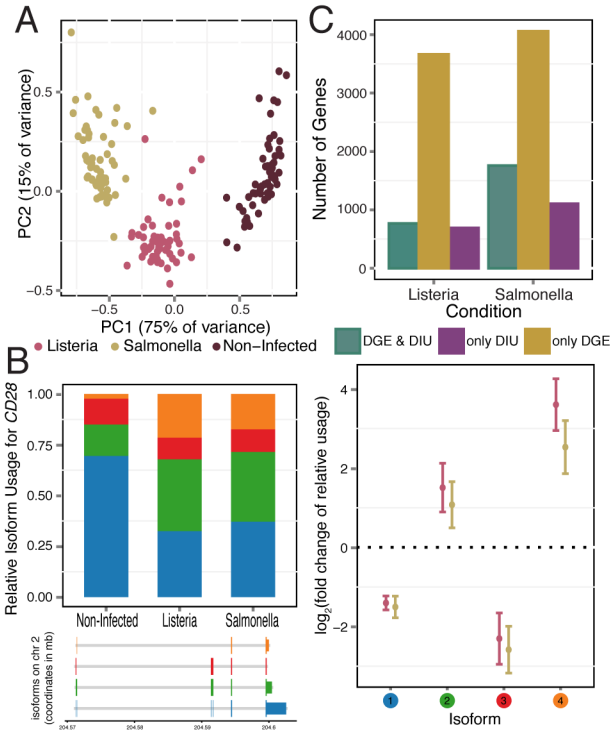

Figure 1. Gene expression and isoform proportion differences in response to bacterial infection. (A) Principal component analysis of gene expression data from all samples (PC1 and PC2 on the *x*- and *y-axis*, respectively). (B) *ADORA3*, a gene with significant changes in isoform usage upon infection with *Listeria* and *Salmonella*. For each *ADORA3* isoform in response to infection, plotted are the average relative isoform usages across samples (*left panel*) and corresponding fold changes (*right panel*; $\log_2$ scale; with standard error bars). Isoforms are ordered by relative abundance in non-infected samples, and colored circles (*right panel*) correspond to colors in barplot (*left panel*). (C) Number of genes showing only DIU, only DGE, and both DIU and DGE upon infection with *Listeria* and *Salmonella*, (11,353 genes tested).

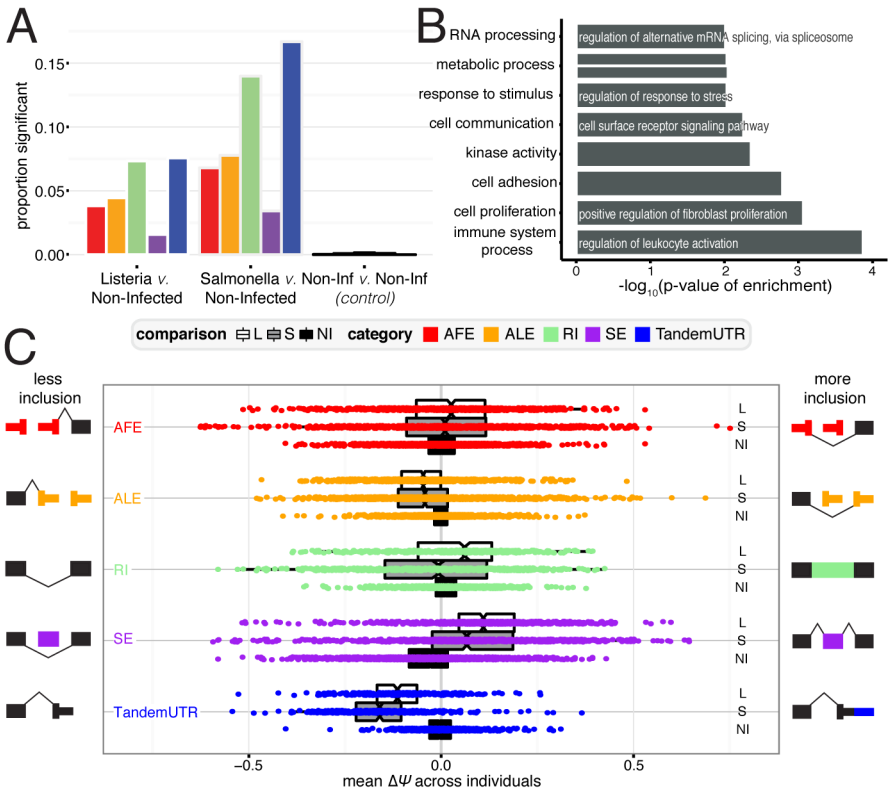

Figure 2. RNA processing changes in response to bacterial infection. (A) Proportion of events for RNA processing category that are significantly changing after infection with *Listeria* (*left*), *Salmonella* (*middle*), or variation between non-infected samples as a control (*right*). Numbers indicate the number of significant changes per category. (B) Significantly Gene Ontology categories for genes with any significant RNA processing change (FDR ≤ 10%). (C) Distribution of ΔΨ values for each RNA processing category. Negative values represent less inclusion, while positive values represent more inclusion, as defined by the schematic exon representations.

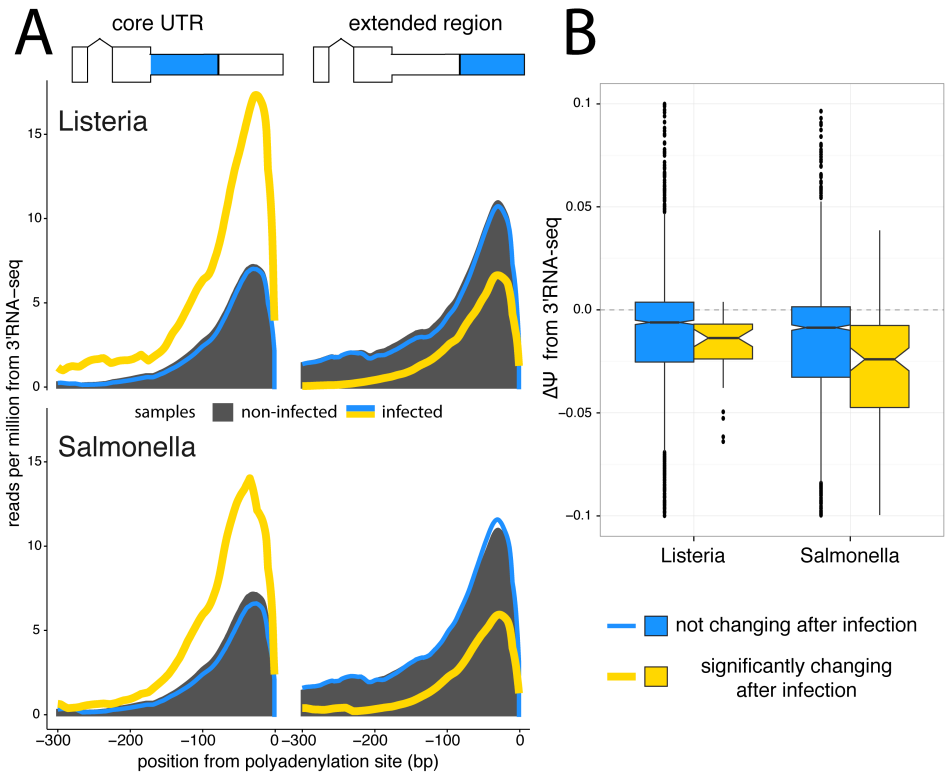

Figure 3. 3'RNA sequencing shows increased usage of upstream polyadenylation sites upon infection. (A) Meta-gene distributions of 3'RNA-seq read densities at the upstream polyA sites (core regions, *left*) and downstream polyA sites (extended regions, *right*) of Tandem 3' UTRs after infection with *Listeria* or *Salmonella* (*top* and *bottom*, respectively). Shown are the read distributions for non-infected samples across all Tandem 3' UTRs (*black*) and infected samples at Tandem 3' UTRs that significantly change after infection (*yellow*) or show no change after infection (*blue*), as called by the RNA-seq data. (B) Distribution of ΔΨ values calculated from 3'RNA-seq data for Tandem 3' UTRs. We observe significant shifts ($P < 2.2 \times 10^{-16}$ for both *Listeria* and *Salmonella*) towards negative ΔΨ values in Tandem UTRs that are identified as significantly changing in RNA-seq data (*yellow*) relative to Tandem UTRs without any change after infection (*blue*).

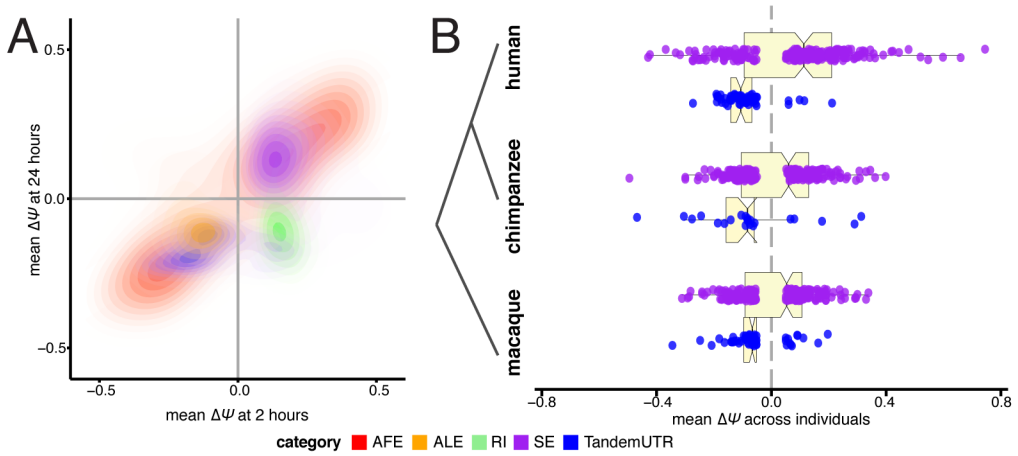

860
861
862 **Figure 4. Directed shifts in RNA processing persist across time, stimulus**
863 **conditions, and closely related species.** (A) Correlations between ΔΨ values after
864 2 hours of infection (*x-axis*) and ΔΨ values after 24 hours of infection (*y-axis*),
865 presented as density plots per RNA processing category in contrasting colors.
866 Plotted are events that are significant after 2 hours of either *Listeria* or *Salmonella*
867 infection. (B) Distributions of ΔΨ values for skipped exons (*purple*) and
868 TandemUTRs (*blue*) following infection of whole blood cells with
869 lipopolysaccharide, assessed in human (*top*), chimpanzee (*middle*) and rhesus
870 macaque (*bottom*) individuals (*N=6* per species). We observe prominent global
871 shifts in isoform distributions in human and macaque (SE_{human} *P=0.003*,
872 $TandemUTR_{human}$ $P=2.4\times10^{-13}$; $SE_{macaque}$ *P=0.05*, $TandemUTR_{macaque}$ $P=8.8\times10^{-6}$) with a
873 more modest trend observed in chimpanzee, potentially due to poor transcript
874 annotations in the chimpanzee genome ($SE_{chimpanzee}$ *P=0.26*, $TandemUTR_{chimpanzee}$
875 *P=0.002*). All p-values were calculated using a Student's t-test testing deviation from
876 a mean of zero.
877

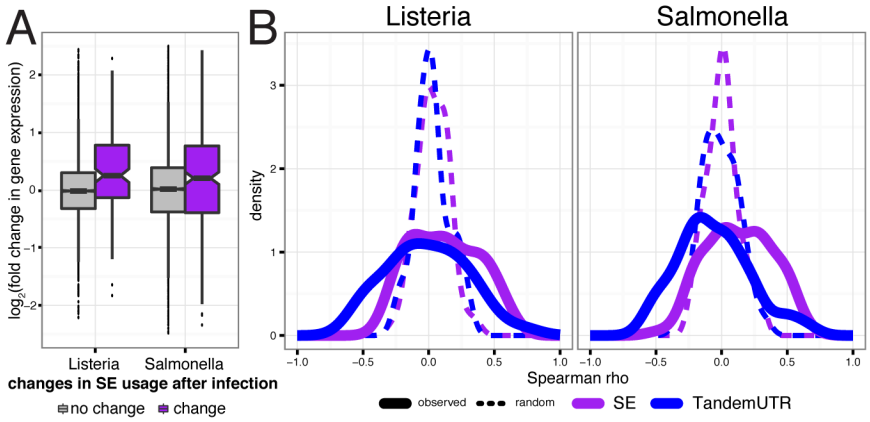

Figure 5. Relationship between RNA processing changes and gene expression changes. (A) Distribution of fold changes in gene expression (*y-axis*, $\log_2$ scale) for genes with significant skipped exon changes after infection (*purple*) and genes with no change after infection (*gray*). (B) Distribution of Spearman correlations between ΔΨ and fold change in gene expression across 60 individuals per gene (*solid line*), for genes with only one annotated alternative event and significantly changed SE usage (*purple*; n_L = 46 genes and n_S = 97 genes) or tandem UTR usage (*blue*; n_L = 36 genes and n_S = 86 genes). Dotted lines show distribution of the correlation coefficients after permuting ΔΨ values.

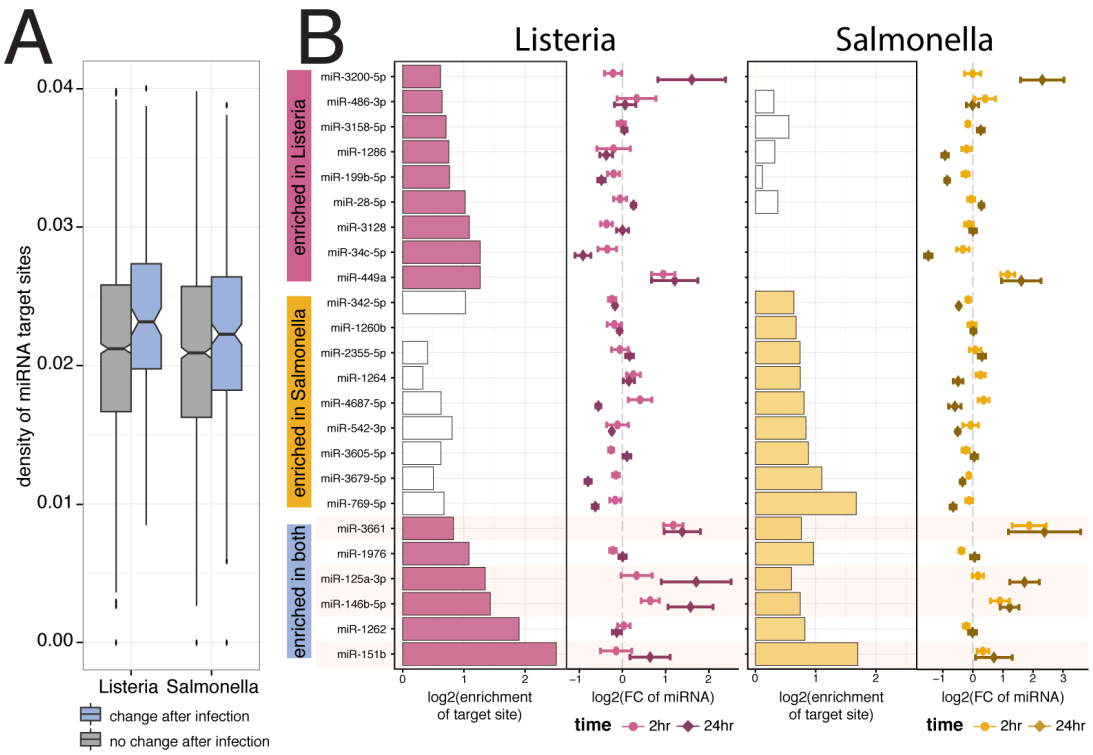

892

893

894 **Figure 6. Tandem 3' UTR shortening allows evasion of regulation by miRNAs.**
895 (A) Distribution of frequency of miRNA target sites per nucleotide in the extended
896 regions of Tandem UTRs that either show no change after infection (*grey*) or
897 significantly change after infection (*blue*). (B) Significantly enriched miRNA target
898 sites (FDR ≤ 10%, |FC| > 1.5) in the extended regions of significantly changing
899 Tandem UTRs after infection with *Listeria*-only (*top*), with *Salmonella*-only (*middle*),
900 or both bacteria (*bottom*). For each bacteria, the barplots in the left panels show the
901 fold enrichment (*x-axis*, $\log_2$ scale) of target sites in the extended regions. White bars
902 represent non-significant enrichments. Panels on the right show the fold change in
903 miRNA expression (*x-axis*, $\log_2$ scale with standard error bars) after either 2 hours
904 of infection (*light colors*) or 24 hours of infection (*dark colors*).

905